Particle Accelerators, 1994, Vol. 45, pp. 149–165
Reprints available directly from the publisher
Photocopying permitted by license only

IMAGE EFFECTS FOR BUNCHED BEAMS IN AXISYMMETRIC SYSTEMS*

CHRISTOPHER K. ALLEN, NATHAN BROWN and MARTIN REISER

Institute for Plasma Research, University of Maryland,
College Park, MD. 20742, USA

(Received 20 September 1993; in final form 14 March 1994)

We analyze the longitudinal image force on bunched beams in cylindrical conducting tubes assuming ellipsoidal uniform density. Numerical and approximate analytic solutions for the potential and electric field of such bunches are presented. It is found that the total self fields are linear only when the bunch length is less than the pipe diameter. The fields become highly nonlinear as the bunch length increases beyond the pipe diameter. Using the equivalent linear model for the longitudinal electric field, we calculate the geometry factor for different bunch sizes. Other bunch geometries are also considered.

KEY WORDS: Electromagnetic field calculations, impedances

1 INTRODUCTION

Image forces resulting from the presence of a beam pipe can play an important role in the dynamics of bunched beams. In previous treatments of longitudinal instabilities and of the behavior of bunched beams, the longitudinal image forces have been assumed linear in axial distance and independent of radial distance. The longitudinal self fields, including image effects, have usually been represented by a geometry factor g, used as a constant of proportionality between longitudinal self electric field and the derivative of line charge density. It is the purpose of this paper to investigate these longitudinal self fields in detail and incorporate our findings into the geometry factor model.

It is known that a uniform ellipsoidal charge distribution yields linear internal fields in free space,[1,2,3] and it has been previously assumed that these fields are also approximately linear in the presence of metallic boundaries.[4] However, we find through numerical simulation and analytic approximations that the fields are linear only for short bunches. The longitudinal field becomes more hyperbolic as the bunch length increases.

* Research supported by ONR and DOE.

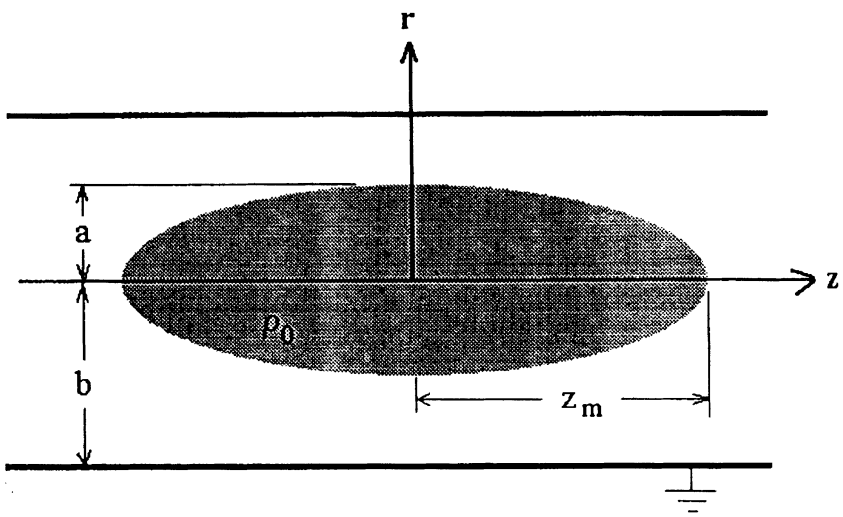

FIGURE 1: Ellipsoidal Bunch in Cylindrical Pipe.

To our knowledge, there is no simple analytical solution for the potential distribution of a uniform ellipsoidal bunch in a cylindrical pipe, our primary focus in this paper. We have obtained numerical solutions for this case using the method of moments,[5] also referred to as the charge-density (or integral) method.[6] We also develop some approximate analytic results. In addition the results for some charge distributions which may be solved analytically are presented. Both of these results rely on the Green's function technique for the inversion of Poisson's equation.[7]

We compare these results to the geometry factor ("g-factor") model for the longitudinal electric fields. This model was originally developed to treat perturbations on continuous cylindrical beams and has been extended to the bunched beam case. We provide some modifications to the model in order to make it consistent with our findings.

2 BUNCHED BEAM MODEL

We model the bunched beam as a uniform axisymmetric ellipsoid with constant charge density ρ_0. The ellipsoid has radial semi-axis a, longitudinal semi-axis z_m and is centered inside a conducting pipe of radius b. The situation is depicted in Figure 1. We explicitly consider only the case of a prolate ellipsoid ($z_m > a$) but the results are readily extended for the oblate case.

We make all field calculations in the beam frame, so we need only consider Poisson's equation. Thus, for relativistic beams it is necessary to Lorentz transform the solution into the laboratory frame. We need to solve the following system of equations:

$$\nabla^2\phi(r,z) = -\frac{\rho(r,z)}{\epsilon_0} \quad \text{for } r \in [0,b],\ z \in (-\infty,+\infty),$$

$$\phi(b,z) = 0 \quad \text{for } z \in (-\infty,+\infty), \tag{1}$$

where ϕ is the electrostatic self potential and ρ is the volume charge density. The pair (r, z) denote the radial and axial coordinates in a cylindrical coordinate system. We assume that the beam is centered in the pipe, which is considered to be a perfect conductor. The charge density may be written explicitly as

$$\rho(r,z) = \begin{cases} \rho_0 & \text{if } r \in \left[0, a\sqrt{1-z^2/z_m^2}\right],\ z \in [-z_m, z_m] \\ 0 & \text{otherwise} \end{cases} \tag{2}$$

for the uniform ellipsoid. Once the potential is known, the electric field $\mathbf{E}$ is given by $-\nabla\phi$ which, along with any external forces, dictates the beam dynamics. Throughout this analysis we assume that there exist linear external focusing forces which confine the bunch.

We may separate the total self potential ϕ into two components, the free-space potential ϕ_{fs} and the image potential ϕ_i; that is

$$\phi(r,z) = \phi_{fs}(r,z) + \phi_i(r,z). \tag{3}$$

The free space potential is known analytically. For points inside the ellipsoid, it is[3]

$$\phi_{fs}(r,z) = \frac{\rho_0 z_m^2}{2\epsilon_0}\left[1-\xi^2(1-M_E)\right] - \frac{\rho_0}{2\epsilon_0}\left[\frac{1-M_E}{2}r^2 + M_E z^2\right], \tag{4}$$

where

$$\xi = \sqrt{1-a^2/z_m^2},$$

$$M_E = \frac{1-\xi^2}{\xi^2}\left[\frac{1}{2\xi} ln \frac{1+\xi}{1-\xi} - 1\right]. \tag{5}$$

Note that the first term for $\phi_{fs}(r,z)$ is simply a constant. Also note that ϕ_{fs} depends quadratically both on r and z and, consequently, the fields are linear inside the ellipsoid. Thus, for linear focusing fields the uniform ellipsoid is a stationary distribution in free space. In order to continue the analysis of beam dynamics, we need to determine the image fields inside the ellipsoid. Before proceeding, however, we introduce the g-factor model for the longitudinal electric field.

3 GEOMETRY FACTOR MODEL FOR E_Z

The general method of modeling the longitudinal effects uses the so-called g-factor.[4,8,9,10,11,12] In this model the longitudinal electric field inside the bunch is defined in terms of the line charge density $\lambda(z)$ as

$$E_z(z) = -\frac{g}{4\pi\epsilon_0}\frac{d\lambda(z)}{dz}, \tag{6}$$

where

$$\lambda(z) = 2\pi \int_0^b \rho(r, z) r dr, \tag{7}$$

and g is the g-factor which is dependent upon the geometry of the system. Thus, for the uniform ellipsoid of Equation (2) we find

$$E_z(z) = g\frac{a^2}{z_m^2}\frac{\rho_0}{2\epsilon_0}z \tag{8}$$

inside the bunch. We may find the radial self field through the divergence equation $\nabla \cdot \mathbf{E} = \rho/\varepsilon_0$ as

$$E_r(r) = \left(1 - \frac{g}{2}\frac{a^2}{z_m^2}\right)\frac{\rho_0}{2\epsilon_0}r. \tag{9}$$

We see that both fields are linear in their respective coordinates. It is the goal of this paper to determine the value for g. In the free space case, we may find g simply by comparing the derivative of (4) with respect to z and Equation (8). Denoting the free space g-factor as g_0, we have

$$g_0 = 2\frac{z_m^2}{a^2}M_E = \frac{2}{1-\xi^2}M_E. \tag{10}$$

Before proceeding, it is convenient to introduce some definitions. In the forthcoming discussion it is found that the true E_z is not a linear function of z. We may still use the definition (6) by assuming that g is a function of r and z, i.e. $g = g(r, z)$. Also, note that for the ellipsoidal bunch of Equation (2), the total charge Q is given by

$$Q = \frac{4}{3}\pi a^2 z_m \rho_0. \tag{11}$$

Using Equation (8) and the above value we define the function g as follows:

$$g(r, z) \equiv \frac{8\pi\epsilon_0 z_m^3}{3Q}\frac{E_z(r, z)}{z}. \tag{12}$$

We also denote $g(0, 0)$ as simply $g(0)$.

We can express the nonlinear results in terms of an "equivalent linear beam" in which the form of (8) is still valid, but the geometry factor is redefined. First we introduce the familiar weighted average for any function f of r and z:

$$\langle f(r,z)\rangle \equiv 2\pi \int\int f(r,z)\rho(r,z)rdrdz\,. \tag{13}$$

Thus, $\langle z\rangle$ and $\langle z^2\rangle$ are the first and second moments of z about the distribution $\rho(r,z)$. Next we define an average g-factor which is appropriate for the collective particle behavior,

$$\bar{g} \equiv \frac{8\pi\epsilon_0 z_m^3}{3Q}\frac{\langle zE_z(r,z)\rangle}{\langle z^2\rangle} = \frac{\langle z^2 g(r,z)\rangle}{\langle z^2\rangle} = \frac{8\pi\epsilon_0 z_m^3}{3Q}\frac{\int\int zE_z(r,z)\rho(r,z)rdrdz}{\int\int z^2\rho(r,z)rdrdz}\,. \tag{14}$$

The first order electric field within the bunch is then given by $E_z = \left(3Q/8\pi\epsilon_0 z_m^3\right)\bar{g}z$. This is a least-squares linear fit to the actual field. It represents an equivalent linear model to the nonlinear field.

4 NUMERICAL RESULTS

As previously mentioned, the numerical results were obtained using a moment method technique. Briefly, this consists of discretizing the cylindrical pipe into triangular finite elements. A uniform surface charge is assumed on each triangle, the magnitude of which is to be determined. Thus, the system consists of a (piecewise constant) surface charge distribution $\sigma(b,z)$ and a volume charge distribution $\rho(r,z)$. The total potential anywhere in space is the superposition of the individual potentials from each charge distribution. The potential for $\rho(r,z)$ is known analytically,[1] therefore we must determine $\sigma(b,z)$ in order to match the boundary condition $\phi(b,z) = 0$. In the method of moments, the coefficients for σ are selected to meet this criterion in the least squares sense. All numerical results are given for the ellipsoidal distribution (2).

The potential and electric field were computed numerically for a range of parameter values. The ratio z_m/a was varied over the interval 1 to 20 for the values b/a = 1.5, 2, 3, and 5. Figures 2a through 2f illustrate the general trend for the axial potential and z electric field as z_m/a is increased; this is for the case $b/a = 3$. The radial semi-axis a was held at 1 cm throughout. The total bunch charge was $10^{-11}C$, thus for each case $\rho_0 = 3\times 10^{-11}C/4\pi a^2 Z_m$. Note the change in axis scales, especially for the z-axis.

For z_m less than b, the electric field is essentially linear; yet, as bunch length increases beyond this point the fields become increasingly nonlinear. From the numerical calculations it is possible to compute the g-factor, which we find to be a function of both z_m/a and b/a. Both $g(0)$ and $\bar{g}$ vary as a function of eccentricity and both approach a limiting value as $z_m/a \to \infty$. We find that as $z_m/a \to \infty$,

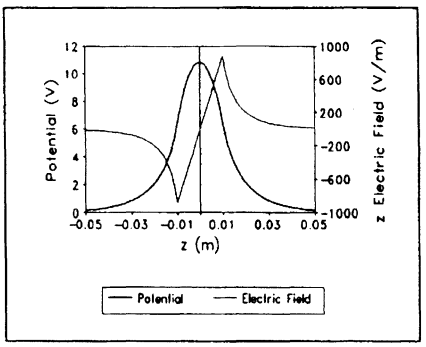

a: $z_m = a$

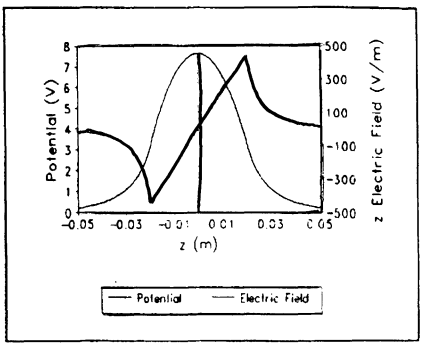

b: $z_m = 2a$

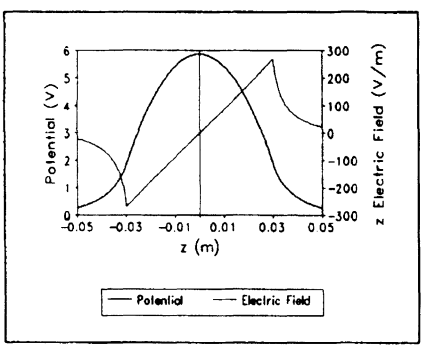

c: $z_m = 3a$

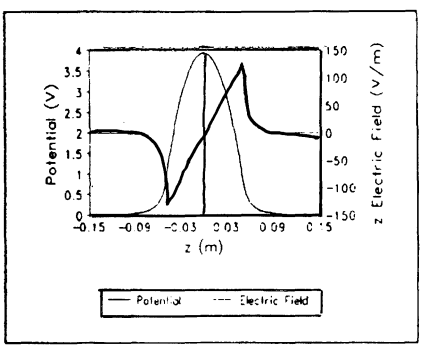

d: $z_m = 5a$

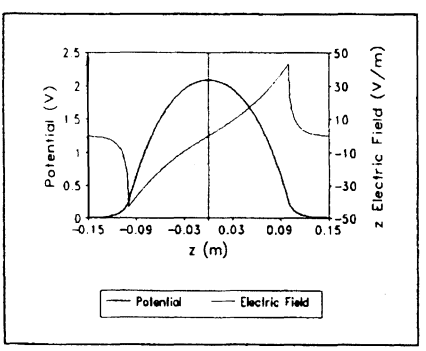

e: $z_m = 10a$

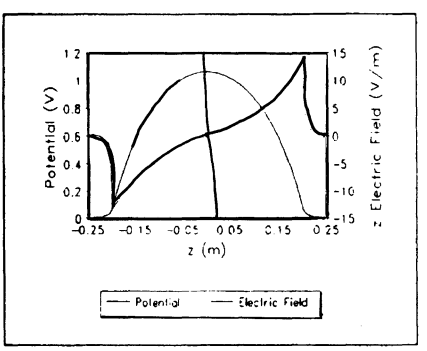

f: $z_m = 20a$

FIGURE 2: Axial Potential and Longitudinal Electric Field for b/a=3.

TABLE 1: Geometry Factors versus z_m/a and b/a

z_m/a	$b/a = 1.5$		$b/a = 2$		$b/a = 3$		$b/a = 5$		
	$g(0)$	$\bar{g}$	$g(0)$	$\bar{g}$	$g_{(0)}$	$\bar{g}$	$g(0)$	$\bar{g}$	g_0
1	0.58	0.59	0.63	0.63	0.66	0.66	0.66	0.66	0.67
1.5	0.80	0.85	0.93	0.94	1.01	1.01	1.04	1.04	1.05
2	0.91	1.02	1.14	1.18	1.31	1.31	1.37	1.37	1.39
3	0.94	1.21	1.35	1.48	1.73	1.76	1.90	1.90	1.96
4	0.89	1.30	1.41	1.65	1.98	2.05	2.29	2.30	2.41
5	0.85	1.38	1.40	1.74	2.12	2.24	2.57	2.60	2.79
7.5	0.81	1.38	1.39	1.86	2.19	2.52	2.96	3.08	3.52
10	0.81	1.40	1.39	1.93	2.19	2.63	3.11	3.34	4.06
15	0.81	1.40	1.39	1.97	2.20	2.72	3.19	3.58	4.84
20	0.81	1.41	1.39	1.97	2.20	2.77	3.21	3.68	5.40

$$g(0) \to 2ln\left(\frac{b}{a}\right),$$

$$\bar{g} \to 0.6 + 2ln\left(\frac{b}{a}\right). \tag{15}$$

We also find that the longitudinal field is essentially independent of radius except at the ends of the bunch.

Values of $g(0)$ and $\bar{g}$ along with g_0 are listed in Table 1. for several different values of b/a. These values are plotted as a family of curves in Figure 3. Note that our results differ significantly from the results found in the literature,[9,11,12] where the fields are assumed to be linear and various values of g are used, including $2ln(b/a)$, $1/2 + 2ln(b/a)$, and $1 + 2ln(b/a)$. These are considered to be valid only in the long bunch limit. We also note in this context that the g-factors for longitudinal perturbations in the long wavelength limit differ from the g-factors associated with bunched beams.[8]

5 ANALYTICAL RESULTS

5.1 Green's Function

Green's function $G(r, z; r', z')$ for an axisymmetric charge distribution $\rho(r', z')$ may be computed by solving Poisson's equation for a unit ring of charge (in $r - z$ space)

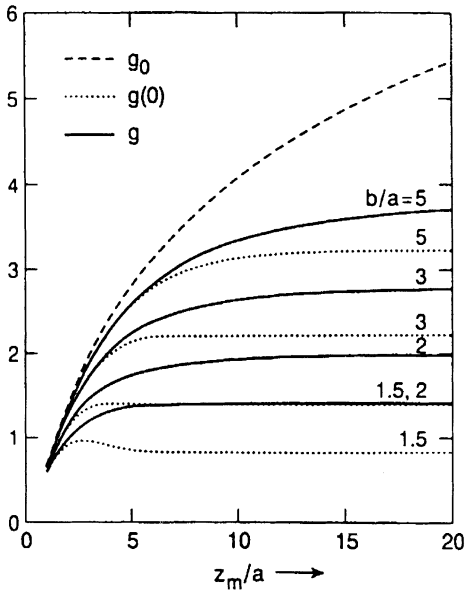

FIGURE 3: Geometry Factor versus z_m/a and b/a, where $g=\bar{g}$.

located at source point (r', z'). The resulting equation becomes

$$\nabla^2 G(r, z) = -\frac{\delta(r - r')\delta(z - z')}{\epsilon_0 r} \qquad r \in [0, b],\ z \in [-\infty, +\infty]$$

$$G(r, z) = 0 \qquad r = b,\ z \in [-\infty, +\infty] \tag{16}$$

This equation may be solved by standard techniques.[7] In particular, we solve (16) by expanding $G(r, z)$ in terms of the orthogonal set of Bessel functions $\{J_0(\alpha_n r/b) : n = 1, 2, \ldots$ and $J_0(\alpha_n) = 0\}$ where the coefficients are functions of z. By substituting this expansion into (16), then taking inner products with $J_0(\alpha_m r/b)$ we obtain an equation for each coefficient. Solving for each coefficient, the desired Green's function is given by the infinite summation

$$G(r, z; r', z') = \frac{1}{\epsilon_0 b} \sum_{n=1}^{\infty} \frac{J_0\left(\frac{\alpha_n}{b} r\right) J_0\left(\frac{\alpha_n}{b} r'\right)}{\alpha_n J_1^2(\alpha_n)} e^{-\frac{\alpha_n}{b}|z - z'|}, \tag{17}$$

where the unprimed coordinates indicate field points and the primed coordinates denote source points. The solution $\phi(r, z)$ to Equation (1) for any axisymmetric $\rho(r, z)$ may now be written as

$$\phi(r, z) = \int_{-\infty}^{+\infty} \int_0^b G(r, z; r', z')\rho(r', z')r' dr' dz' \tag{18}$$

5.2 *Uniform Ellipsoidal Charge Distribution*

By applying (18) to the distribution (2) we end up with the incomplete solution

$$\phi(r,z) = \frac{\rho_0 a}{\epsilon_0} \sum_{n=1}^{\infty} \frac{J_0\left(\frac{\alpha_n}{b} r\right)}{\alpha_n^2 J_1^2(\alpha_n)} \int_{-z_m}^{+z_m} \sqrt{1 - \frac{z'^2}{z_m^2}}\, J_1\left(\frac{\alpha_n}{b} a \sqrt{1 - \frac{z'^2}{z_m^2}}\right) e^{-\frac{\alpha_n}{b}|z-z'|} dz' \tag{19}$$

Although there is no known analytic solution to the above integral we can make some approximations. Consider the case where $z \in [-z_m, +z_m]$. As $z_m \to \infty$ the exponent in the above integral behaves much like a Dirac delta function around z, since the other expressions vary slowly in comparison. Thus, the radical and the Bessel function may be pulled from the integral and evaluated at $z' = z$. If $|z| > z_m$ then we evaluate them at $z' = z_m$. The resulting expression becomes

$$\phi(r,z) = \begin{cases} \dfrac{2\rho_0 ab}{\epsilon_0} \sqrt{1 - \frac{z^2}{z_m^2}} \displaystyle\sum_{n=1}^{\infty} \dfrac{J_0\left(\frac{\alpha_n}{b} r\right) J_1\left(\frac{\alpha_n a}{b} \sqrt{1 - \frac{z^2}{z_m^2}}\right)}{\alpha_n^3 J_1^2(\alpha_n)} \\ \quad \bullet \left(1 - e^{-\frac{\alpha_n z_m}{b}} \cosh\left(\frac{\alpha_n}{b} z\right)\right) & \text{for } z \in [-z_m, z_m] \\ 0 & \text{for } |z| > z_m \end{cases} \tag{20}$$

The total electric field for the long bunch approximation is found by differentiating (20). We have

$$E_z(r,z) = \begin{cases} \dfrac{2\rho_0 a^2}{\epsilon_0} \dfrac{z}{z_m^2} \displaystyle\sum_{n=1}^{\infty} \dfrac{J_0\left(\frac{\alpha_n}{b} r\right) J_0\left(\frac{\alpha_n a}{b} \sqrt{1 - \frac{z^2}{z_m^2}}\right)}{\alpha_n^2 J_1^2(\alpha_n)} \left(1 - e^{-\frac{\alpha_n z_m}{b}} \cosh\left(\frac{\alpha_n}{b} z\right)\right) \\ \quad + \dfrac{2\rho_0}{\epsilon_0} \sqrt{1 - \frac{z^2}{z_m^2}} \displaystyle\sum_{n=1}^{\infty} \dfrac{J_0\left(\frac{\alpha_n}{b} r\right) J_1\left(\frac{\alpha_n a}{b} \sqrt{1 - \frac{z^2}{z_m^2}}\right)}{\alpha_n^2 J_1^2(\alpha_n)} e^{-\frac{\alpha_n z_m}{b}} \sinh\left(\frac{\alpha_n}{b} z\right) & \text{for } z \in [-z_m, z_m] \\ 0 & \text{for } |z| > z_m \end{cases} \tag{21}$$

Notice that the field is dominated by the top expression since the exponent is small at the center of the bunch while the radical is small at the ends. Note also that it is

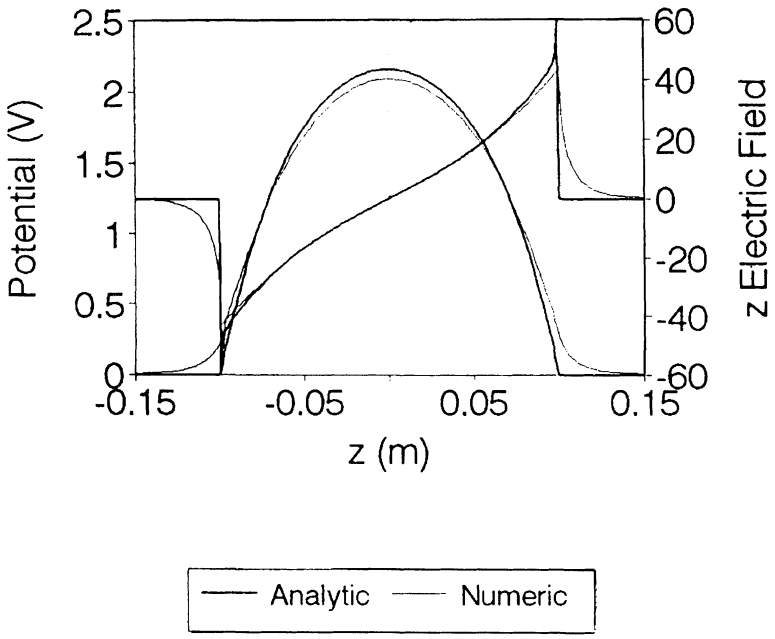

FIGURE 4: Ellipsoid Analytic Approximation.

possible to obtain a better approximation by adding the first order correction terms to (20) and (21). For the potential $\phi(r, z)$ in Equation (20), these terms appear as follows:

$$\frac{\rho_0}{\epsilon_0}\sum_{n=1}^{\infty}\frac{J_0\left(\frac{\alpha_n}{b}r\right)}{\alpha_n^2 J_1^2(\alpha_n)}\frac{\partial}{\partial z'}\left[a\sqrt{1-\frac{z^2}{z_m^2}}\,J_1\left(\frac{\alpha_n}{b}a\sqrt{1-\frac{z^2}{z_m^2}}\right)\right]_{(z'=z)}$$

$$\cdot\int_{-z_m}^{+z_m}(z-z')\,e^{-\frac{\alpha_n}{b}|z-z'|}dz'. \tag{22}$$

Equations (20) and (21) are plotted against the numerical results in Figure 4. The summation was truncated at 20 terms and the test case of $z_m = 10$ cm, $b = 3$ cm, $a = 1$ cm and $Q = 10^{-11}C$ was used. Note the spikes in the analytic curve for E_z; this is because (21) is mildly singular a $z = z_m$.

A convenient identity may be derived by applying (18) to a uniform cylindrical distribution (see section 5.3). By allowing $z_m \to \infty$ and comparing with the known potential solution for the continuous beam case, we arrive at the following relation:

$$\sum_{n=1}^{\infty} \frac{J_1\left(\frac{\alpha_n}{b}a\right) J_0\left(\frac{\alpha_n}{b}r\right)}{\alpha_n^3 J_1^2(\alpha_n)} = \begin{cases} \frac{a}{8b}\left(1 + 2ln\left(\frac{b}{a}\right) - \frac{r^2}{a^2}\right) & r \in [0, a] \\ \frac{a}{8b}\left(2ln\left(\frac{b}{a}\right)\right) & r \in [a, b] \end{cases} \tag{23}$$

Within the distribution we may apply this identity to determine a simplified expression for the central potential. Neglecting the exponential terms in (20) we have

$$\phi(r, z) = \frac{\rho_0 a^2}{4\epsilon_0}\left[\left(1 + 2ln\left(\frac{b}{a}\right) - ln\left(1 - \frac{z^2}{z_m^2}\right)\right)\left(1 - \frac{z^2}{z_m^2}\right) - \frac{r^2}{a^2}\right]. \tag{24}$$

Thus we may compute the central field to be

$$E_z(r, z) = \frac{\rho_0 a^2}{2\epsilon_0 z_m^2} 2ln\left(\frac{b}{a}\frac{1}{\sqrt{1 - (z^2/z_m^2)}}\right) z. \tag{25}$$

This is the same expression one would obtain by solving Poisson's equation in the long bunch limit (i.e. neglecting $\partial^2/\partial z^2$). Note that not even the central field is linear.

The above expression also confirms Equation (15) for $g(0)$, since $g(0) \to 2ln(b/a)$ as $z \to 0$. We may get an approximate value for $\bar{g}$ by using expression (25) in Equation (14). The resulting analytic approximation is given by $\bar{g} \to 0.68 + 2ln(b/a)$. This value is an upper bound on $\bar{g}$ since (25) blows up at $z = \pm z_m$. Equation (25) is, however, a reasonably accurate approximation to the fields everywhere else in the bunch, as Figure 5 demonstrates for the same test case.

5.3 *Uniform Cylindrical Charge Distribution*

Equation (1) may be solved exactly for the uniform cylinder in terms of an infinite summation of Bessel functions. This distribution is given by the following:

$$\rho(r, z) = \begin{cases} \rho_0 & \text{if } r \in [0, a],\ z \in [-z_m, +z_m] \\ 0 & \text{otherwise} \end{cases} \tag{26}$$

The resulting potential for this distribution is

$$\phi(r, z) = \begin{cases} \frac{2\rho_0 ab}{\epsilon_0} \sum_{n=1}^{\infty} \frac{J_1\left(\frac{\alpha_n a}{b}\right) J_0\left(\frac{\alpha_n}{b}r\right)}{\alpha_n^3 J_1^2(\alpha_n)} \left(1 - e^{-\frac{\alpha_n z_m}{b}} \cosh\left(\frac{\alpha_n}{b}z\right)\right) & \text{for } z \in [-z_m, +z_m] \\ \frac{2\rho_0 ab}{\epsilon_0} \sum_{n=1}^{\infty} \frac{J_1\left(\frac{\alpha_n a}{b}\right) J_0\left(\frac{\alpha_n}{b}r\right)}{\alpha_n^3 J_1^2(\alpha_n)} \sinh\left(\frac{\alpha_n z_m}{b}\right) e^{-\frac{\alpha_n}{b}|z|} & \text{for } |z| > z_m. \end{cases} \tag{27}$$

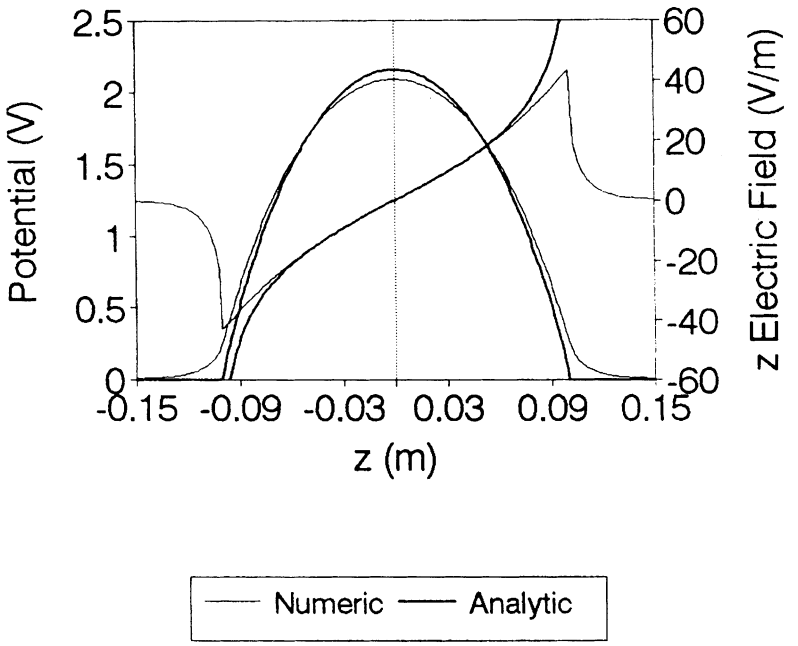

FIGURE 5: Simplified Analytic Approximation.

Inside the distribution, we may apply (23) to display the central potential which is independent of z, as one would expect.

$$\phi(r,z) = \frac{\rho_0 a^2}{4\epsilon_0}\left[1 + 2ln\left(\frac{b}{a}\right) - \frac{r^2}{a^2}\right] + \frac{2\rho_0 ab}{\epsilon_0}\sum_{n=1}^{\infty}\frac{J_1\left(\frac{\alpha_n a}{b}\right)J_0\left(\frac{\alpha_n}{b}r\right)}{\alpha_n^3 J_1^2(\alpha_n)}e^{-\frac{\alpha_n z_m}{b}}\cosh\left(\frac{\alpha_n}{b}z\right) \tag{28}$$

Here the central potential (first term) and the fringing potential (summation) are shown explicitly. The electric field is given by the expression

$$E_z(r,z) = \begin{cases} \frac{2\rho_0 a}{\epsilon_0}\sum_{n=1}^{\infty}\frac{J_1\left(\frac{\alpha_n a}{b}\right)J_0\left(\frac{\alpha_n}{b}r\right)}{\alpha_n^2 J_1^2(\alpha_n)}e^{-\frac{\alpha_n z_m}{b}}\sinh\left(\frac{\alpha_n}{b}z\right) & \text{for } z \in [-z_m, +z_m] \\ \frac{2\rho_0 a}{\epsilon_0}\sum_{n=1}^{\infty}\frac{J_1\left(\frac{\alpha_n a}{b}\right)J_0\left(\frac{\alpha_n}{b}r\right)}{\alpha_n^2 J_1^2(\alpha_n)}e^{-\frac{\alpha_n}{b}|z|}\sinh\left(\frac{\alpha_n z_m}{b}\right)sgn(z) & \text{for } |z| > z_m \end{cases} \tag{29}$$

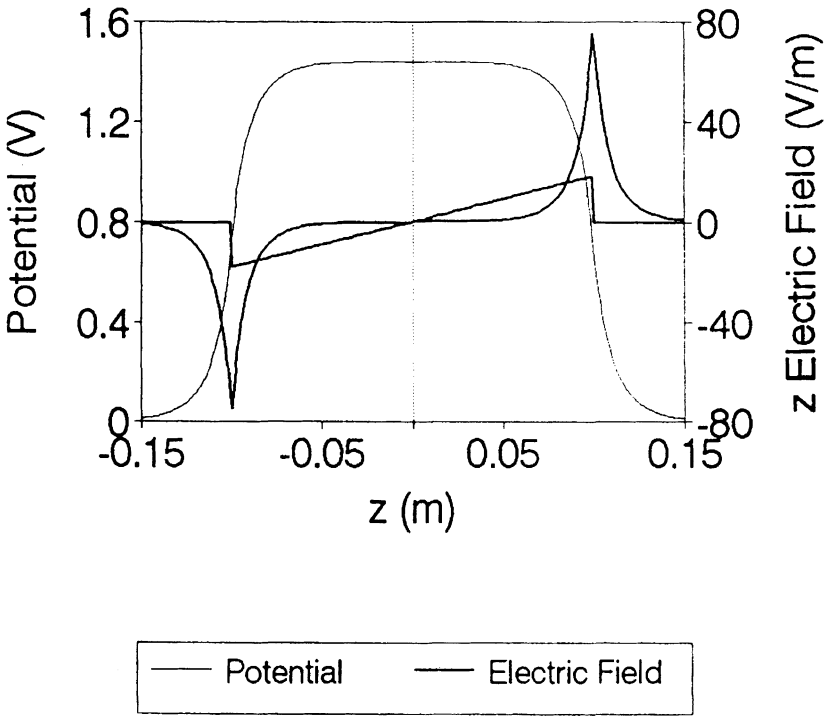

FIGURE 6: Uniform Cylinder, b/a=3, z_m/a=10.

In Figure 6, this field is plotted, along with the r.m.s value of E_z, for our test case $z_m = 10$ cm, $b = 3$ cm, $a = 1$ cm, and $Q = 10^{-11}C$. We see clearly that almost all the field is in the regions of the head and tail of the distribution. Essentially we have only fringe fields.

In case of the uniform cylinder $g(r, z)$ is essentially undefined, since $d\lambda/dz$ is zero almost everywhere. Physically, this idea is seen in the above equation for E_z which consists entirely of the fringing effect. Thus, the central field is zero. However, $\bar{g}$ may still be defined. The result of this calculation is

$$\bar{g} = \frac{8b^2}{a^2} \sum_{n=1}^{\infty} \frac{J_1^2\left(\frac{\alpha_n a}{b}\right)}{\alpha_n^4 J_1^2(\alpha_n)} \left[\cosh\left(\frac{\alpha_n z_m}{b}\right) - \frac{b}{\alpha_n z_m} \sinh\left(\frac{\alpha_n z_m}{b}\right)\right] e^{-\frac{\alpha_n z_m}{b}} \tag{30}$$

which in the limit $z_m \to \infty$ becomes $1/4 + ln(b/a)$.

5.4 *Parabolic Cylindrical Charge Distribution*

This distribution consists of a cylinder of charge with a parabolic density in z. Precisely, we have

$$\rho(r,z) = \begin{cases} \rho_0\left(1-\frac{z^2}{z_m^2}\right) & \text{if } r \in [0,a],\ z \in [-z_m,+z_m] \\ 0 & \text{otherwise} \end{cases} \tag{31}$$

This distribution has been treated previously by Irani using similar techniques.[13] The solution to this distribution is

$$\phi(r,z) = \begin{cases} \frac{2\rho_0 ab}{\epsilon_0}\sum_{n=1}^{\infty}\frac{J_1\left(\frac{\alpha_n a}{b}\right)J_0\left(\frac{\alpha_n}{b}r\right)}{\alpha_n^3 J_1^2(\alpha_n)}\left[\left(1-\frac{z^2}{z_m^2}\right)-\frac{2b^2}{\alpha_n^2 z_m^2}+\right. \\ \left.\left(\frac{2b}{\alpha_n z_m}-\frac{2b^2}{\alpha_n^2 z_m^2}\right)e^{-\frac{\alpha_n z_m}{b}}\cosh\left(\frac{\alpha_n}{b}z\right)\right] \quad \text{for } z \in [-z_m, z_m] \\ \frac{2\rho_0 ab}{\epsilon_0}\sum_{n=1}^{\infty}\frac{J_1\left(\frac{\alpha_n a}{b}\right)J_0\left(\frac{\alpha_n}{b}r\right)}{\alpha_n^3 J_1^2(\alpha_n)}\left[\frac{2b}{\alpha_n z_m}\cosh\left(\frac{\alpha_n z_m}{b}\right)-\right. \\ \left.\frac{2b^2}{\alpha_n^2 z_m^2}\sinh\left(\frac{\alpha_n z_m}{b}\right)\right]e^{-\frac{\alpha_n}{b}|z|} \quad |z| > z_m \end{cases} \tag{32}$$

which yields an electric field

$$E_z(r,z) = \begin{cases} \frac{4\rho_0 ab}{\epsilon_0}\sum_{n=1}^{\infty}\frac{J_1\left(\frac{\alpha_n a}{b}\right)J_0\left(\frac{\alpha_n}{b}r\right)}{\alpha_n^3 J_1^2(\alpha_n)}\left[\frac{z}{z_m^2}-\left(\frac{1}{z_m}+\frac{b}{\alpha_n z_m^2}\right)e^{-\frac{\alpha_n z_m}{b}}\sinh\left(\frac{\alpha_n}{b}z\right)\right] \\ \qquad\qquad \text{for } z \in [-z_m, z_m] \\ \frac{4\rho_0 ab}{\epsilon_0}\sum_{n=1}^{\infty}\frac{J_1\left(\frac{\alpha_n a}{b}\right)J_0\left(\frac{\alpha_n}{b}r\right)}{\alpha_n^2 J_1^2(\alpha_n)} \\ \bullet\left[\frac{1}{z_m}\cosh\left(\frac{\alpha_n z_m}{b}\right)-\frac{b}{\alpha_n z_m^2}\sinh\left(\frac{\alpha_n z_m}{b}\right)\right]e^{-\frac{\alpha_n}{b}|z|}sgn(z) \text{ for } |z| > z_m. \end{cases} \tag{33}$$

The central potential can be determined from Equation (32). Inside the charge distribution it is given by the expression

$$\phi(r,z) = \frac{\rho_0 a^2}{4\epsilon_0}\left(1-2ln\left(\frac{b}{a}\right)-\frac{r^2}{a^2}\right)\left(1-\frac{z^2}{z_m^2}\right) \tag{34}$$

This is also the total potential in the limit $z_m \to \infty$. Note that this is the distribution which is most accurately described by the original g-factor model.

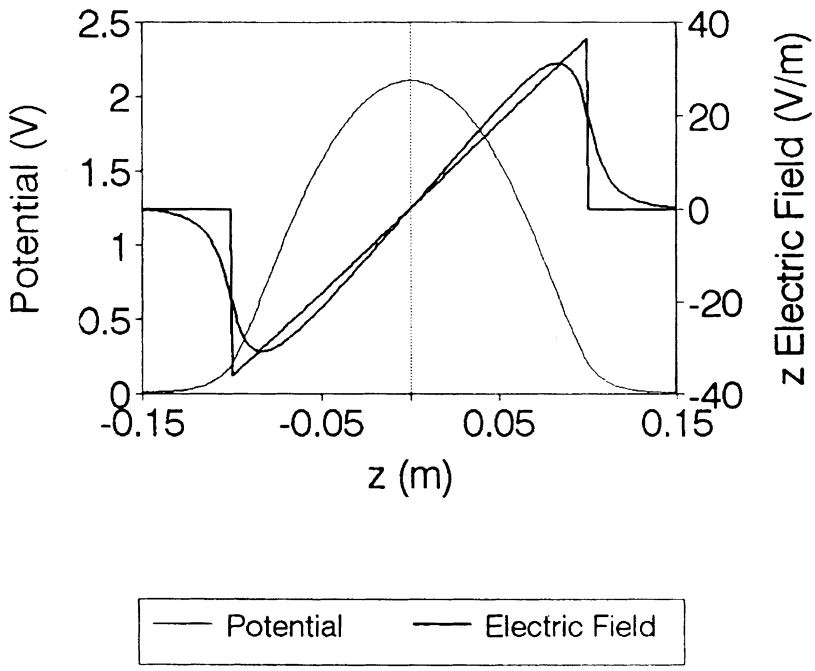

FIGURE 7: Parabolic Cylinder, b/a=3, z_m/a=10.

From these results it is possible to determine the respective g-factors. We have the following:

$$g(0) = 1 + 2ln\left(\frac{b}{a}\right)$$

$$\bar{g} = \frac{240b^2}{a^2}\sum_{n=1}^{\infty}\frac{J_1^2\left(\frac{\alpha_n a}{b}\right)}{\alpha_n^4 J_1^2(\alpha_n)}\left\{\frac{1}{15} + \left(\frac{b}{\alpha_n z_m^2} + \frac{b^2}{\alpha_n^2 z_m^3}\right)\left[\frac{3b}{\alpha_n z_m}\cosh\left(\frac{\alpha_n z_m}{b}\right)\right.\right.$$

$$\left.\left. - \left(1 + \frac{3b}{z_m^2}\right)\sinh\left(\frac{\alpha_n z_m}{b}\right)\right] e^{-\frac{\alpha_n z_m}{b}}\right\} \tag{35}$$

$$\bar{g} \to \frac{1}{2} + 2ln\left(\frac{b}{a}\right) \qquad \text{as } z_m \to \infty$$

Figure 7 shows the potential and z electric field for our test case of the previous sections. The r.m.s. z electric field is also shown.

6 CONCLUSION

The image fields of bunched beams are generally nonlinear. Our results are contrary to previous works where (6) was used for any bunch length greater than b and where g is constant with values ranging from $2ln(b/a)$ to $1 + 2ln(b/a)$. We see that for $z_m \gg b$ the g-factor does indeed reach an asymptotic value independent of z_m, yet (6) is invalid (i.e. the field is quite nonlinear). On the other hand, for short bunches $z_m \ll b$ the form of (6) is valid (i.e. linear fields) however the g-factor is dependent upon z_m. Thus, the use of the g-factor model requires some scrutiny.

The applicability of g seems to be divided into three regions. When z_m/a is much less than b/a we are at liberty to use the free space value for g (i.e. g_0). In this case the pipe dimensions are much larger than the bunch dimensions and the image field has little effect. In the other extreme, when z_m/a is much larger than b/a, the effect of the fringe field is small compared to that of the central field. As such, we may use the asymptotic expressions for g. Between these two extremes we have a transition region where the central fields and the fringe fields are comparable. Accordingly, g is a function of both z_m/a and b/a and there are no simple expressions governing this behavior.

Throughout the analysis we implicitly assumed the existence of linear focusing fields to confine the bunch. We then treated the bunch as an equivalent uniform ellipsoidal distribution which produces linear self fields. It was found that in the presence of a beam pipe the true uniform ellipsoid generates nonlinear self fields. The actual distribution will of course adjust itself in order to maintain equilibrium with the linear external forces. We are currently investigating the behavior of these self consistent distributions. These results and the correlations with our present work will be presented in a future paper.

In relativistic situations, one must Lorentz transform the fields into the laboratory frame. Since this constitutes a scale contraction in the axial direction, this transformation simply results in replacing z and z_m by γz and γz_m in all relevant equations. Also, the derivative of the line-charge density transforms as $(\partial\lambda/\partial z)_{\text{beam}} \rightarrow (1/\gamma^2)(\partial\lambda/\partial z)_{\text{lab}}$, hence a factor $1/\gamma^2$ must be added to the leading coefficients of Equation (6).

REFERENCES

1. O.D. Kellogg, *Foundations of Potential Theory*, (Dover, NY, 1953) pp. 192–194.
2. R.L. Gluckstern, *Linear Accelerators*, (eds.) P. Lapostolle and A. Septier (Amsterdam: North Holland, 1967) p. 827.
3. I.M. Kapchinsky, *Theory of Resonance Linear Accelerators* (Harwood Academic Publishers, New York, 1985) Chapt. 3.1.
4. D. Neuffer, *IEEE Trans. on Nuclear Science*, **NS-26** (1979) 3031.
5. R.F. Harrington, *Field Computation by Moment Methods* (Krieger, Malabar, FL, 1968).
6. M. Szilagyi, *Electron and Ion Optics* (Plenum Press, New York, NY, 1988) pp. 137–143.
7. I. Stakgold, *Green's Functions and Boundary Value Problems* (Wiley, NY, 1979).
8. M. Reiser, *Theory and Design of Charged Particle Beams* (Wiley, 1994) Chapt. 5.4.7, Chapt. 6.3.2.
9. S. Hansen, H.G. Hereward, A. Hofmann, K. Hübner, and S. Myers, *IEEE Trans. on Nuclear Science*, **NS-22**(3) (1975) pp. 1381–1384.
10. A. Faltens, E.P. Lee, and S.S. Rosenblum, *J. Appl. Phys.*, **61**(12) (1987) pp. 5219–5221.

11. J.G. Wang, D.X. Wang, and M. Reiser, *Appl. Phys. Lett.*, **62**(6) (1993) pp. 645–647.

12. T.J.P. Ellison, S.S. Nagaitsev, M.S. Ball, D.D. Caussyn, M.J. Ellison, and B.J. Hamilton, *Phys. Rev. Lett.*, **70**(6) (1993), pp. 790–793.

13. A.A. Irani, in *Proceedings of the Heavy Ion Fusion Workshop, BNL*, Report #BNL-50769 (1977), pp. 124–126.